

ANTINEOPLASTIC AGENTS. CCLII (*).
ISOLATION AND STRUCTURE OF HALISTATIN 2
FROM THE COMOROS MARINE SPONGE *Axinella carteri* ()**

GEORGE R. PETTIT^a (°), FENG GAO^a, DENNIS L. DOUBEK^a, MICHAEL R. BOYD^b, ERNEST HAMEL^c, RUOLI BAI^c, JEAN M. SCHMIDT^a, LARRY P. TACKETT^a and KLAUS RÜTZLER^d

^a) Cancer Research Institute and Department of Chemistry, Arizona State University, Tempe, AZ 85287-1604, USA

^b) Laboratory of Drug Discovery Research and Development, DTP, DCT, National Cancer Institute, Frederick Cancer Research and Development Center, Frederick, MD 21702-1201, USA

^c) Laboratory of Molecular Pharmacology, DTP, DCT, National Cancer Institute, Bethesda, MD 20892, USA

^d) National Museum of Natural History, Smithsonian Institution, Washington, DC 20560, USA

Summary — An intensive long-term investigation of marine organisms as sources of new anticancer drugs has led to the isolation and structural elucidation (primarily by high-field NMR and mass spectrometry) of halistatin 2, **7b**, a new polyether macrolide of the halipyrans-type, from the Western Indian Ocean sponge *Axinella* cf. *carteri* (Dendy). Halistatin 2 ($1.4 \times 10^{-6}\%$ yield) was accompanied by the closely related, and also strongly antineoplastic, halistatin 1 (**6b**, $1.3 \times 10^{-6}\%$ yield), halichondrin B (**6a**, $6.1 \times 10^{-6}\%$ yield) and homohalichondrin B (**7a**, $4.3 \times 10^{-6}\%$ yield). Halistatin 2, like halichondrin B and homohalichondrin B, caused the accumulation of cells arrested in mitosis, inhibited tubulin polymerization, and inhibited the binding of radiolabelled vinblastine and GTP to tubulin.

A great number of ancient marine invertebrate species in the Phyla Bryozoa, Mollusca and Porifera were well established in the earth's oceans over one billion years ago. Certainly such organisms explored trillions of biosynthetic reactions in their evolutionary chemistry to reach present levels of cellular organization, regulation and defense. Marine sponges have changed minimally in physical appearance for nearly 500 million years, suggesting a very effective chemical evolution in response to changing environmental conditions for at least that time period. Some recognition of the potential for utilizing biologically potent marine animal constituents was recorded in Egypt about 2,700 BC¹, and by 200 BC sea hare extracts were being used in Greece for medicinal purposes². Such considerations, combined with the general observation that marine organisms (especially invertebrates and sharks) rarely develop cancer, led one of us (GRP) in 1965-6 to initiate the first systematic investigation of marine animal and plant anticancer constituents.

By 1968¹ we had obtained ample evidence, based on the U.S. National Cancer Institute's key experimental cancer systems, that certain marine organisms would provide new and structurally novel antineoplastic and/or cytotoxic agents. Analogous considerations suggested that marine organisms could also provide effective new drugs for other

severe medical challenges, such as viral diseases. Furthermore, marine organisms were expected to contain potentially useful drug candidates (and biochemical probes) of unprecedented structural types, that would have eluded discovery by contemporary techniques of medicinal chemistry. Fortunately, these expectations have been realized in the intervening period³⁻¹¹. Illustrative of these successes (cf. 1-5) are our discoveries of the bryostatins^{6,12-14}, dolastatins^{15,16}, and cephalostatins¹⁷ where five members of these series of remarkable anticancer drug candidates are either now in human clinical trial (e.g., 1) or preclinical development.

A major component of our vigorous efforts for over two decades¹ has been directed at marine sponge antineoplastic and/or cytotoxic biosynthetic products. A number of unusual polyether macrolides, peptides and heterocyclic compounds have been uncovered¹⁸⁻²³. Isolation and structural elucidation of a new, strongly cytotoxic macrolide (halistatin 2, **6b**) will now be described.

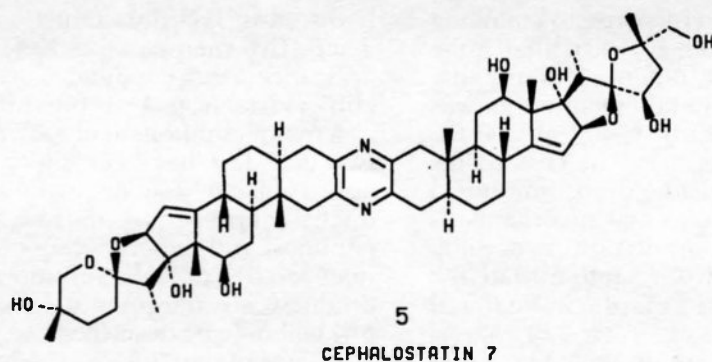
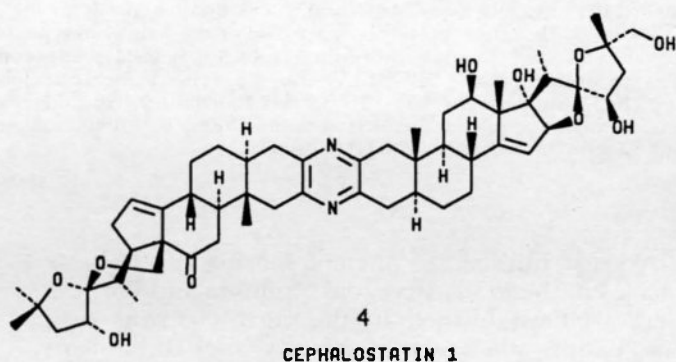
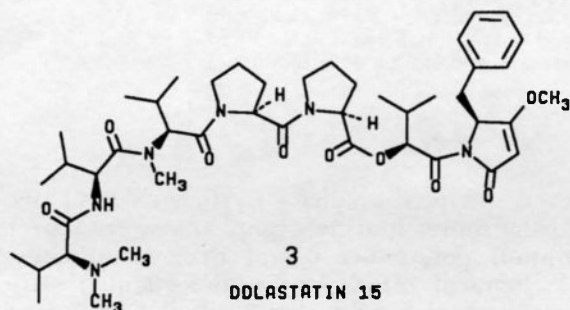
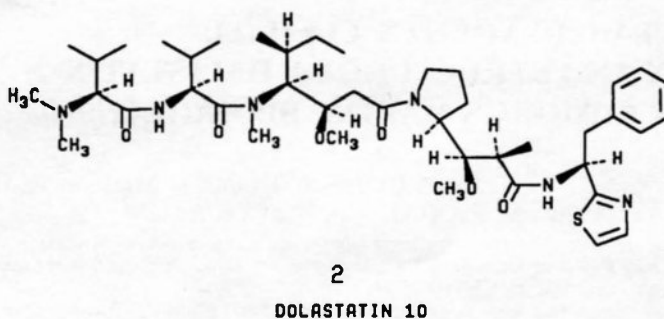
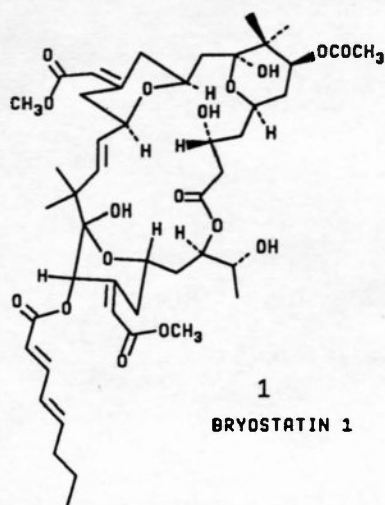
As part of our 1987-9 expedition in the Republic of the Comoros we evaluated marine sponge species in the order Axinellida. Specimens of the cosmopolitan *Axinella* cf. *carteri* (Dendy) were found to yield extracts with potent antineoplastic properties (cures observed in the U.S. National Cancer Institute murine *in vivo* P388 lymphocytic leukaemia, PS system). Given the extraordinary level of antineoplastic activity, the presence of halichondrin-type constituents was suspected, such as we identified in new *Axinella* species collected (1979) in the Western Pacific (Palau)¹⁸ and in the Western Indian Ocean²⁴.

A 1989 recollection (1,080 kg wet wt) of the erect orange sponge *Axinella carteri*²⁵ (in methanol) was divided into two (600 kg and 480 kg) amounts. Both

(*) For contribution CCLI refer to: G.R. PETTIT, J.K. SRIRANGAM, D.L. HERALD, K.L. ERICKSON, D.L. DOUBEK, J.M. SCHMIDT, L.P. TACKETT, G.J. BAKUS, *J. Org. Chem.*, 57, 7217 (1991).

(**) Presented at the Seventh International Symposium on Marine Natural Products, Capri, Italy, July 5-10, 1992.

(°) To whom correspondence should be addressed.

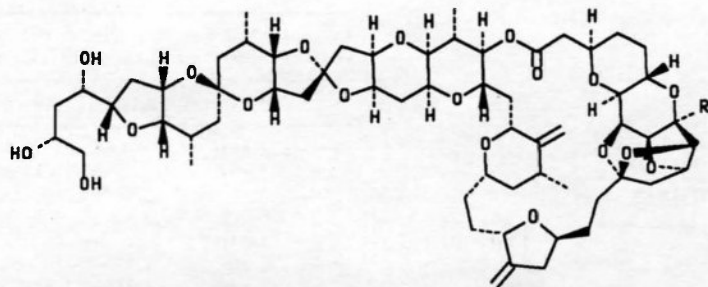


portions were extracted with methanol-dichloromethane, and the chlorocarbon fraction was partitioned in methanol-water (9:1→3:2) between hexane→dichloromethane⁴. The resulting PS cell line active (ED₅₀ 0.26 μg/ml) dichloromethane fraction was then separated (see the scheme) by a series of gel permeation and partition column chromatographic steps on Sephadex LH-20, followed by HPLC on RP-8 reversed phase silica gel. Investigation of the 600 kg amount of the orange sponge was first directed at fractions that might contain new polyether antineoplastic agents, and the 480 kg amount was used for the further scale-up procurement (for extensive

biological studies) of halichondrin B, **6a^e**, and homohalichondrin B, **7a**.

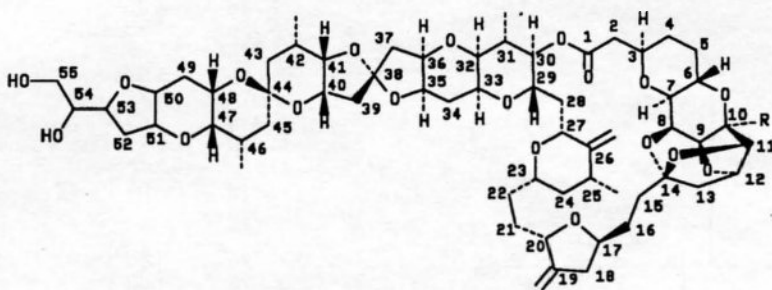
The halichondrins are a series of antineoplastic polyether macrolides first isolated (in microgram amounts) from the relatively rare marine sponge *Halichondria okadai*²⁶. Halichondrin B, **6a**, was reported to have potent *in vitro* activity against the mouse B-16 melanoma (IC₅₀ 9.3 × 10⁻⁶ ng/ml) and *in vivo* activity against the murine B-16, P-388 and L-1210 tumors²⁶. Results of our *in vitro* and *in vivo*

(^e) Selected (in March, 1992) by the U.S. National Cancer Institute for preclinical development.



6 a, HALICHONRIN B, R = H

b, HALISTATIN 1, R = OH



7 a, HOMOHALICHONRIN B, R = H

b, HALISTATIN 2, R = OH

evaluations against human cancer cell lines¹⁸ and xenografts have given further evidence of very strong cytotoxic and antineoplastic effects. These polyethers have been found to inhibit tubulin assembly¹⁹ and to cause the accumulation of cells arrested in mitosis at nanomolar concentrations.

The bioassay (PS cell line) guided separation of *Axinella cf. carteri* afforded (1.4×10^{-6} % yield) the new and very active macrolide halistatin 2, **7b**. In addition, halichondrin B, **6a**, homohalichondrin B, **7a**, and halistatin 1, **6b**, were isolated in 6.1×10^{-6} , 4.3×10^{-6} and 1.3×10^{-6} % yields, respectively. Since characterization of halichondrin-type macrolides requires in-depth 2D-NMR studies at high field it became necessary to further interpret the ¹H- and ¹³C NMR spectra of halistatin 1, **6b**, and the synopsis that now follows further augments our earlier structural determination²⁴.

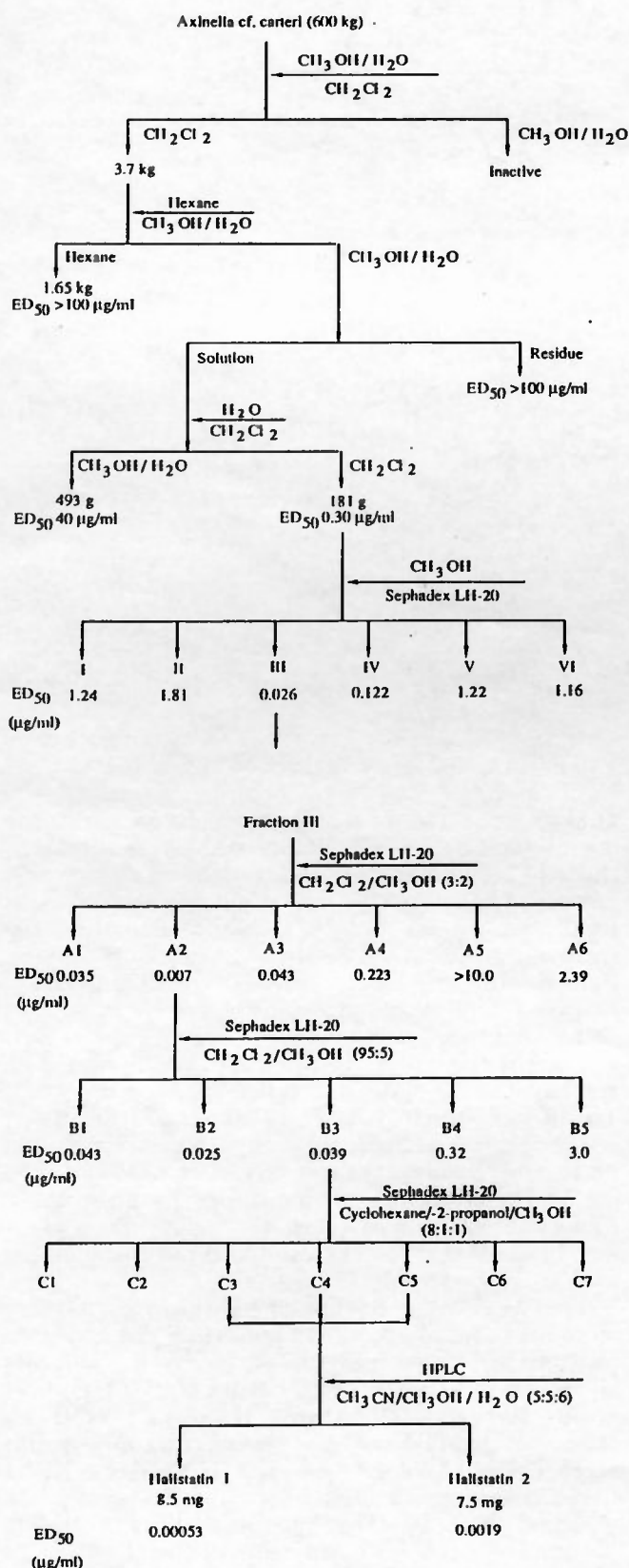
Further studies of halistatin 1 employing 2D NMR techniques confirmed the structure. The ¹³C signal at δ 103.73 (C-10) showed correlation with ¹H signals at δ 3.74 (H-9), 4.25 (H-11), 4.23 (H-8), and 4.74 (H-12); the ¹³C signals at δ 87.64 (C-11) showed cross peaks at δ 3.74 (H-9), 2.12 (H-13), 4.74 (H-12); the ¹³C signal at δ 110.83 (C-14) showed cross peaks at δ 4.25 (H-11), 4.74 (H-12), 1.97 and 2.12 (H-13), and δ 4.23 (H-8). Analysis of NOE results with halistatin 1 supported assignment of the stereochemistry. When the signal for H-7 was irradiated, the signals for H-9 and H-8 were enhanced. Irradiation of the signal for H-9 enhanced the H-7 signals and irradiation of the H-12 signal enhanced the H-11 and a H-13 signal (δ

1.97). Thus, the asymmetric centres at C-7 to C-14 were assigned the same configuration as the analogous centres of halichondrin B, **6a**. Since the overall high-field NMR data were also very similar to those of halichondrin B, the remaining asymmetric centres of halistatin 1 were assumed to be analogous to the parent **6a** molecule. As noted earlier, the hydroxyl group at C-10 was assigned the α -orientation. Dreiding molecular models indicated that a β -hydroxyl group was sterically unlikely in such a condensed ring system.

The structure of halistatin 2, **7b**, was assigned on the basis of 2D NMR and other spectroscopy data. The IR spectrum of halistatin 2 indicated absorptions corresponding to hydroxyl groups, an ester carbonyl and double bonds at respectively 3358, 1734 and 1653 cm^{-1} . The FAB-MS of halistatin 2 suggested a molecular formula of $\text{C}_{61}\text{H}_{86}\text{O}_{20}$, using the peak at m/z 1145 $[\text{M}+\text{Li}]^+$ as corresponding to a calculated molecular weight of 1138.

The ¹H NMR spectrum of halistatin 2 was very similar to that of homohalichondrin B, **7a**, reported previously²⁶, especially the four methyl doublet signals at δ 1.08 ($J=6.4$ Hz), 1.04 ($J=7.1$ Hz), 0.94 ($J=7.0$ Hz) and 0.93 ($J=6.8$ Hz)²⁶ (see table 1). However, detailed analyses revealed significant differences from δ 3.4-4.8 ppm. The ¹H NMR and ¹H-¹H COSY data suggested that a free hydroxyl group was attached to C-10. The chemical shifts, coupling patterns and coupling constants of the H-8 to H-13 signals were basically the same as those of halistatin 1, **6b**. For example, the signal at δ 4.73 (triplet, $J=4.6$

SCHEME

TABLE 1 - HALISTATIN 2, 7b, NMR ASSIGNMENTS (CD_3OD SOLUTION WITH TETRAMETHYLSILANE AS INTERNAL STANDARD)^a

	^{13}C (100 MHz)	XHCorr. (400 MHz)	HMBC (500 MHz)
1	172.86p		H-2, H-30
2	41.19p	2.55 dd(10,18); 2.46 brd(18)	
3	75.00n	3.91	H-2
4	31.61p		
6	71.20n	4.45	H-7, H-8
7	78.84n	3.05 dd(1.8,9.7)	H-8
8	75.16n	4.24	H-7, H-9
9	79.77n	3.74 brd(4.4)	H-8, H-11, H-12
10	103.75p		H-8, H-9, H-11, H-12
11	87.64n	4.25	H-9, H-12, H-13
12	82.29n	4.73 t(4.6)	H-9, H-11, H-13
13	49.00p	2.13; 1.96 dd(5,13)	
14	110.83p		H-8, H-11, H-12, H-13
16	29.37p	2.17; 1.40	H-18
17	77.18n	4.07	H-18
18	39.75p	2.80 brm; 2.32	H-19a
19	153.16p		H-18, H-17, H-19a
19a	105.65p	5.05 brs; 5.00 brs	H-18
20	76.07n	4.45	H-19a
23	75.45n	3.69 brt(10)	
24	44.96p	1.72; 1.02	H-25a
25	37.22n	2.32	H-25a, H-24, H-26a
25a	18.41n	1.08 d(6.4)	H-24
26	153.32p		H-27, H-25, H-25a, H-24, H-26a
26a	104.79p	4.86 brs; 4.80 brs	H-27, H-25
27	75.07n	3.60	H-29, H-26a
28	37.90p	2.25; 1.80	H-29, H-30
29	73.78n	4.23	H-27, H-28
30	77.56n	4.62 dd(4.7,7.6)	H-29, H-31a
31	37.50n	2.05	H-29, H-31a
31a	15.76n	1.04 d(7.1)	H-30, H-31, H-32
32	78.20n	3.20 dd(4.9,6.7)	H-30, H-31a, H-33
33	65.95n	3.88	H-29, H-32
34	30.85p	2.04; 1.80	H-33, H-36
35	76.34n	4.10	H-36
36	78.01n	4.10	H-35
37	45.51p	2.39; 2.00	
38	114.78p		H-36, H-37, H-39, H-40
39	44.84p	2.30; 2.30	
40	72.31n	3.94 brs	H-39, H-41
41	81.06n	3.65 brt(2.8)	H-42a, H-39
42	27.15n	2.36	H-42a, H-43
42a	18.18n	0.94 d(7.0)	H-43
43	38.09p	1.43; 1.33	H-42a, H-41
44	98.14p		H-43
45	38.17p		H-46a, H-47
46	30.14n	2.18	H-46a, H-47
46a	17.65n	0.93 d(6.8)	H-47
47	74.57n	3.11 brd(2.2)	H-46a
48	65.31n	3.57	H-47
49	32.03p	2.10; 1.92	H-48
50	75.81n	3.86	H-48, H-51
51	78.44n	4.01 brs	H-47, H-50
52	37.29p	2.02;	
53	79.87n	4.24	H-55, H-51
54	75.16n	3.49 brdd(5.5,10)	H-55
55	65.18p	3.56 brs; 3.56 brs	

(^a) Chemical shifts, δ , are expressed in ppm, coupling constants (in parentheses) in Hz. Both n and p indicate APT results. The ^{13}C NMR signal for the C-13 was overlapped with solvent signals. Some of the coupling patterns and/or coupling constants were not measured due to overlapping. The other four unassigned ^{13}C NMR signals were at δ 30.09; 31.47; 33.06 and 35.92 for C-5; C-15; C-21 and C-22.

Hz, H-12) was coupled with a signal at δ 4.25 (H-11) and two upfield signals at δ 2.13 and 1.96 (H-13). A signal at δ 4.24 (H-8) was coupled with a broadened

doublet signal at δ 3.74 (H-9), which showed long range coupling with the signal at δ 4.25 (H-11).

In the ^{13}C NMR spectrum, sixty-one carbon signals from halistatin 2 were observed. Among these signals, four were hemiacetal at δ 103.75 (C-10), 110.83 (C-14), 114.78 (C-38) and 98.14 ppm (C-44), as elucidated by the ^1H - ^{13}C correlation and APT spectra. While the C-1 to C-14 signals of halistatin 2 were very similar to the C-1 to C-14 signals of halistatin 1, **6b**, the C-25 to C-55 signals were close to those of the relevant signals of homohalichondrin B, **7a**. In agreement with the assigned structure **7b**, 18 methylene group signals were observed arising from halistatin 2 in the δ 50 to 28 ppm region of the ^{13}C NMR spectrum. Moreover, interpretation of an HMBC spectrum strongly supported the assigned structure. The hemiacetal signal at δ 103.75 (C-10) showed cross peaks with the H-8, H-9, H-11 and H-12 signals and the C-14 carbon signal at δ 110.83 showed cross peaks with the H-8, H-11, H-12 and H-13 signals. The C-10 hydroxyl group was again assigned the α -orientation on the basis of optical rotation ($[\alpha]_D^{25} - 59$) and the NOE difference spectroscopy results (see table 2).

TABLE 2 - THE NOE DIFFERENCE SPECTROSCOPY INTERPRETATION FOR HALISTATINS 1, **6b**, and 2, **7b**. THE SPECTRA WERE RECORDED IN CD_3OD

Signals irradiated	Signals enhanced	
	Halistatin 1, 6b	Halistatin 2, 7b
H-7	H-9, H-8	H-9, H-8
H-9	H-7	H-7
H-12	H-11, H-13	H-11, H-13
H-18		H-17
H-25a		H-26a
H-27	H-30	
H-30	H-27, H-31a	H-31a, H-28
H-31a	H-30	H-26a
H-32		H-31a

Like halistatin 1, the C-10 α hydroxyl-substituted homohalichondrin B (halistatin 2) was of comparable cytotoxic potency (*e.g.*, $\text{GI}_{50} \sim 7 \times 10^{-10} \text{ M}$) to the parent halichondrins **6a** and **7a** when evaluated in the NCI *in vitro* primary screen^{27,28}. Moreover, computerized pattern-recognition analyses²⁹ of the mean graph profiles^{28,29} confirmed the visually apparent (figure) similarities of the screening profiles of the halistatins with halichondrin B. These analyses further demonstrated that the screening profiles of the halistatins/halichondrins were characteristic of a general mechanistic class of tubulin-interactive antimetabolites. The latter class includes such diverse agents as the known clinically active antitumor drugs, vincristine, vinblastine and taxol, as well as new investigational drugs such as dolastatin 10.

Since halichondrin B and homohalichondrin B were found to be antimetabolic agents interfering with the polymerization of purified tubulin and microtubule assembly dependent on microtubule-associated proteins¹⁹, halistatin 2 was evaluated for these activities, and it was compared to halichondrin B isolated from a Palau *Axinella* sp.¹⁸.

With L1210 murine leukaemia cells halistatin 2

and halichondrin B had similar cytotoxicity (IC_{50} values of 0.4 and 0.2 nM, respectively), and both agents caused a significant rise in the mitotic index at cytotoxic concentrations, reaching values as high as 20% for halistatin 2. In the glutamate-induced polymerization of purified tubulin, performed as described previously¹⁹, the two compounds had identical IC_{50} values of $4.9 \pm 0.5 \mu\text{M}$. Halichondrin B has been shown to be a noncompetitive inhibitor of the binding of radiolabelled vinblastine to tubulin and to inhibit nucleotide exchange on tubulin¹⁹. A comparison of halistatin 2 with halichondrin B in these two assays indicated that halistatin 2 had activity comparable to halichondrin B as an inhibitor of vinblastine binding, but that halistatin 2 was superior as an inhibitor of nucleotide exchange. Comparing the two drugs at 5 and 10 μM , halistatin 2 inhibited the binding of radiolabelled vinblastine to tubulin by 51% and 75% at the two concentrations, as compared with 51% and 73% with halichondrin B. For radiolabelled GTP binding to tubulin, the same drug concentrations inhibited the reaction by 17% and 51% with halistatin 2, and by 14% and 18% with halichondrin B. Comparable values obtained previously¹⁹ with halichondrin B did not differ significantly from those obtained in the current studies.

EXPERIMENTAL

GENERAL PROCEDURES

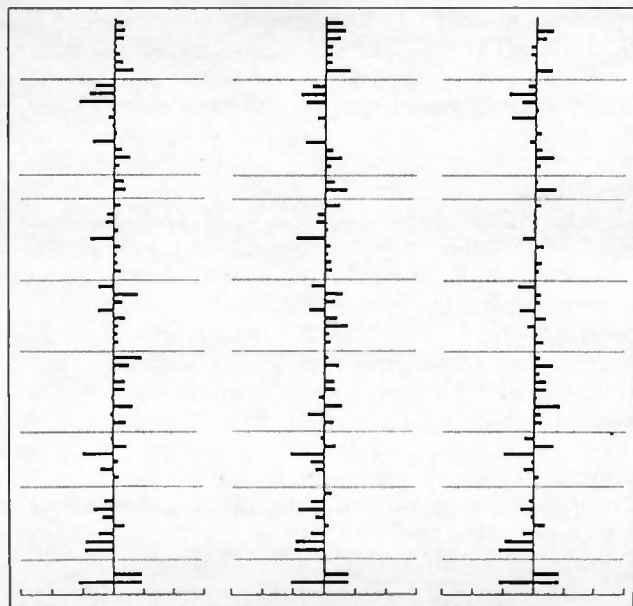
Solvents used for column chromatography were redistilled. Sephadex LH-20, particle size 25-100 μm , used in column chromatographic separation was obtained from Pharmacia Fine Chemicals AB, Uppsala, Sweden. The TLC plates were from Analtech, Inc. The TLC plates were viewed under short-wave (250 nm) UV-light first and then sprayed with ceric sulphate in 3 N sulphuric acid followed by heating at approximately 150 $^\circ\text{C}$. For HPLC separations, the following conditions were used: Phenomenex Preplex RP-8 Reverse Phase semipreparative column (10.0 \times 250 mm, particle size 5-20 μm); acetonitrile-methanol-water (5:5:6) as eluting solvent; Altex 110A pump controlled by Axiom micro-computer; Rainin RI-1 detector, range 32, and time constant 0.25. The flow rate (0.8 or 1.0 ml/min) and sample (1.0 to 4.0 mg) injection varied as noted. The ^1H NMR, APT, ^1H - ^1H COSY, ^1H - ^{13}C COSY, NOE and ^{13}C NMR experiments were carried out using a Bruker AM-400 NMR spectrometer equipped with cryomagnet and ASPECT-300 computer. The HMBC spectra were recorded with a Varian 500 NMR spectrometer. The optical rotations were measured with a Perkin-Elmer 241 polarimeter.

Axinella cf. *carteri* (Dendy)

The orange sponge²⁵ (1080 kg, wet wt.) was recollected in September, 1989 at -27 to -50 m in the Chindini and Foubouni areas of Grande Comore Island (Republic of Comoros). The sponge was preserved in methanol.

SPONGE EXTRACTION AND SOLVENT PARTITION

Part A - The methanol shipping solution from approximately 600 kg (wet wt.) of *Axinella carteri* was decanted and to the solution was added an equal volume of dichloromethane (~600 l) and enough (10-20% by volume) water to provide two phases. The dichloromethane layer was separated and solvent evaporated *in vacuo* to yield the first extract (1.43 kg). To the sponge was added 1:1 dichloromethane-methanol (550 l). After 28 days, water (15% by volume) was added to produce a chlorocarbon phase which was separated and concentrated (*in vacuo*) to obtain the second extract



GI_{50} mean graphs from screening of halistatin 1 (left), halistatin 2 (center) and halichondrin B (right). Each graph is constructed from the averaged GI_{50} 's calculated for each cell line from four separate screenings of each compound. The horizontal scaling bars (bottom of each graph) are marked in increments of $\pm 1 \log_{10}$. The reference centrelines for each graph are located at negative \log_{10} values of 9.15, 9.17 and 9.64 for the left, centre and right graphs, respectively. In each graph the bars projecting to the right of centreline reflect proportionately more sensitive lines; bars projecting to the left of centreline reflect the less sensitive lines.

(1.66 kg). Recovered dichloromethane was combined with the upper layer (methanol/water) to form a dichloromethane-methanol-water solvent mixture (approximately 2:3.8:1.2) that was returned to the sponge to obtain the third dichloromethane extract fraction (607 g) in an analogous manner (18-32 day extraction periods). The combined dichloromethane extract (3.7 kg) was dissolved in a mixture (20 l each) of hexane and 9:1 methanol-water and extracted (six times) with hexane in a 55 l steel container. The hexane fraction was concentrated at 30 °C and then the temperature was raised to 50 °C to remove water. The dark oily residue weighed 1.65 kg. The 9:1 methanol-water solution was filtered (filter paper) and the tan precipitate collected (385 g, ED_{50} 17 $\mu\text{g/ml}$). The solution was diluted to 3:2 by adding 12 l of water and extracted with dichloromethane (20 l, 3 \times). Concentration *in vacuo* gave a 181 g fraction from the chlorocarbon extract and a 493 g fraction from the methanol-water one. Bioassay results (PS ED_{50} 0.30 $\mu\text{g/ml}$) pointed to the dichloromethane residue as the repository of the antineoplastic constituents. The PS cell line active fraction (181 g) was subjected to separation by gel permeation through a Sephadex LH-20 column (15 \times 120 cm) packed in methanol. The column was eluted with methanol (25 l) and fractions were monitored by the P388 cell line bioassay. The active fractions (3) were added to the top of another Sephadex LH-20 column (9 \times 92 cm) in methanol-dichloromethane (3:2) and eluted with the same solvent. Active fractions were further separated by Sephadex LH-20 column (4.5 \times 80 cm) partition chromatography using 95:5 dichloromethane-methanol as eluant. The resulting active fraction was next separated on a Sephadex LH-20 column (2.5 \times 40 cm) using the solvent system 8:1:1 cyclohexane-isopropanol-methanol. Final isolation and purification procedures utilized HPLC to provide 7.5 mg (1.3 $\times 10^{-6}\%$ yield) of halistatin 1, **6b**, and 8.5 mg (1.4 $\times 10^{-6}\%$ yield) of halistatin 2, **7b**. The retention times of halistatin 1 and halistatin 2 were 9.6 and 10.8 min, respectively, at a flow rate of 1.0 ml/min. Halistatin 1, **6b**, corresponded to: $[\alpha]_D^{25} -58$ ($c = 0.57$, CH_3OH); FAB-MS, m/z : 1127 $[\text{M}+\text{H}]^+$; IR (NaCl film): 3356 (OH), 1734 (COOR), 1653 (C=C), 1184, 1080, 1018 cm^{-1} ; and halistatin 2, **7b**, to an amorphous

solid melting at 194.8 °C (Kofler-type hot stage): $[\alpha]_D^{25} -59$ ($c = 0.48$, CH_3OH); FAB-MS, m/z : 1139 $[\text{M}+\text{H}]^+$ ($\text{C}_{61}\text{H}_{86}\text{O}_{20} = 1138$), 1121 $[\text{M}-\text{H}_2\text{O}+\text{H}]^+$; HRFAB-MS, m/z : 1145.5871 $[\text{M}+\text{Li}]^+$, calc for $\text{C}_{61}\text{H}_{86}\text{O}_{20}\text{Li}$ 1145.5872; and IR (NaCl film): 3358 (OH), 1734 (COOR), 1653 (C=C), 1186, 1132, 1078, 1022 cm^{-1} . Tables 1 and 2 show the ^1H - and ^{13}C NMR analyses leading to the structural assignment for halistatin 2.

Part B - The sponge (approximately 480 kg) collected at the same location as discussed above was treated as follows. The methanol shipping solution (140 l) from 120 kg was removed and placed in four 55 l stainless steel containers. Dichloromethane (20 l) was added to each, followed by enough water (approximately 15% by volume) to yield two layers. The lower (dichloromethane) layer was separated and evaporated *in vacuo*, then air-dried to yield 82.1 g of active extract (ED_{50} 0.26 $\mu\text{g/ml}$). This material was dissolved in methanol-water (9:1) and hexane, and partitioned with hexane (yielding 24.5 g, with ED_{50} 1.64 $\mu\text{g/ml}$). Water was added to the methanol-water layer to make a ratio of approximately 3:2, then the solution was filtered to remove the insoluble material (4.4 g, ED_{50} 0.18 $\mu\text{g/ml}$). The solution was partitioned with dichloromethane (three times) to yield 21.7 g of active material (ED_{50} 0.35 $\mu\text{g/ml}$). The inactive methanol-water layer (35 g, ED_{50} 20 $\mu\text{g/ml}$) was discarded.

The active dichloromethane extract (21.7 g) was fractionated on a Sephadex LH-20 column using methanol as solvent. The eluant was monitored by TLC and combined into 7 fractions. The P388 results (ED_{50} 0.011 and 0.035, respectively) suggested that the most active compounds were concentrated in the third and the fourth fractions. Thus, these two fractions were combined (7.7 g) and separated on a Sephadex LH-20 column (9 \times 92 cm) using dichloromethane-methanol (3:2) as eluting solvent. Fractions (22 ml each) were collected (200 total) and combined on the basis of TLC results into six fractions. The first fraction was the most active (ED_{50} 0.017 $\mu\text{g/ml}$).

Parallel treatment and separation of the dichloromethane extract of the shipping solution from 360 kg yielded a similar active fraction ($ED_{50} < 0.01 \mu\text{g/ml}$). These two fractions were combined (2.8 g) and separated on a Sephadex LH-20 column (4.5 \times 80 cm) using the solvent system dichloromethane-methanol (95:5). Again, 22 ml fractions were collected (80 total) and combined on the basis of TLC results yielding four fractions. The third fraction was the most active (ED_{50} 0.00035 $\mu\text{g/ml}$) among the four. Therefore, this fraction was subjected to another Sephadex LH-20 column (1.5 \times 25 cm) separation (cyclohexane-2-propanol-methanol, 8:1:1). A total of 80 fractions (7 ml each) were collected and combined into six fractions. halichondrin B and homohalichondrin B were concentrated in fractions 2 to 4. The final separation of the halichondrins¹⁸ was achieved by semi-preparative HPLC using the conditions outlined at the beginning of the experimental section. Halichondrin B (**6a**, 29.5 mg, 6.1 $\times 10^{-6}\%$ yield) and homohalichondrin B (**7a**, 20.5 mg, 4.3 $\times 10^{-6}\%$ yield) were obtained.

In a related study, we also isolated (using similar isolation procedures) 1.0 mg of halistatin 2, **7b**, from an *Axinella* sp.¹⁸ collected (in 1979) in Palau. By comparison of the high field (400 MHz) ^1H NMR spectra, the two samples were found to be identical.

BIOLOGICAL TESTING; DATA DISPLAY AND ANALYSIS; SCREENING DATA SUMMARY

Freshly isolated halistatin 1, halistatin 2 and halichondrin B were tested in the NCI's human tumor, disease-oriented *in vitro* primary screen, and data calculations performed as described elsewhere²⁷⁻³⁰. The figure is a composite prepared from mean graphs constructed from the averaged GI_{50} values from quadruplicate screenings of each compound. The overall panel mean GI_{50} values were 7.1 $\times 10^{-10}$ M, 6.8 $\times 10^{-10}$ M and 2.3 $\times 10^{-10}$ M for halistatin 1, halistatin 2 and halichondrin B, respectively; standard errors averaged less than 10% of the respective means. Prior comparative testing of homohalichondrin B in the NCI screen had demonstrated approximately equal potency with halichondrin B (data not shown).

The averaged negative \log_{10} GI_{50} values obtained for each cell line with halistatin 2 in the present study are provided as follows, along with the individual cell line identifiers: CCRF-CEM (9.70), HL-60TB (9.80), K-562 (9.64), MOLT-4 (9.39), RPMI-8226 (9.39), SR (9.67); A549/ATCC (8.74), EKVK (8.39), HOP-18 (8.55), HOP-62 (9.16), HOP-92 (8.92), NCI-H226 (9.14), NCI-H23 (9.18), NCI-

H322M (8.52), NCI-H460 (9.42), NCI-H522 (9.70), LXFL 529 (9.35); DMS 114 (9.47), DMS 273 (9.89); COLO 205 (9.66), DLD-1 (8.92), HCC-2998 (8.89), HCT-116 (9.26), HCT-15 (8.26), HT29 (9.34), KM12 (9.27), KM20L2 (9.37), SW-620 (9.40); SF-268 (8.74), SF-295 (9.74), SF-539 (9.49); SNB-19 (8.68), SNB-75 (9.57), SNB-78 (9.92), U251 (9.32), XF 498 (9.37); LOX IMVI (9.30), MALME-3M (9.64), M14 (9.17), M19-MEL (9.51), SK-MEL-2 (9.51), SK-MEL-28 (9.00), SK-MEL-5 (9.74), UACC-257 (8.64), UACC-62 (9.47); IGROV1 (9.05), OVCA-3 (9.55), OVCA-4 (8.11), OVCA-5 (8.74), OVCA-8 (8.89), SK-OV-3 (9.17); 786-0 (9.41), A498 (8.74), ACHN (8.36), CAKI-1 (8.89), RXF-393 (9.32), SN12C (8.74), TK-10 (8.26), UO-31 (8.22).

The very necessary financial assistance for this research was provided by Outstanding Investigator Grant CA 44344-01A1-04 awarded by the Division of Cancer Treatment, National Cancer Institute, DHHS; the Fannie E. Rippel Foundation; the Arizona Disease Control Research Commission; the Robert B. Dalton Endowment Fund; Eleanor W. Libby, the Waddell Foundation (Donald Ware); Virginia Piper; Herbert and Diane Cummings; The Nathan Cummings Foundation, Inc.; Polly Trautman; Lottie Flugal; the Ladies Auxiliary, VFW, Department of Arizona; and the Eagles Art Ehrmann Cancer Fund. Also we are pleased to thank for other helpful assistance the Republic of the Comoros (Damir Ben Ali, Mohammed Chaher, Karl Danga and Bill Carlson), Drs. Jean-Charles Chapuis, Fiona Hogan-Pierson, Ronald A. Nieman, Bruce E. Tucker, Dale R. Sanson and Michael D. Williams, Ms. Denise Nielsen Tackett, Mrs. Kim M. Weiss, Mr. Lee Williams, the U.S. National Science Foundation (Grants CHE-8409644 and BBS-88-04992) and the NSF Regional Instrumentation Facility in Nebraska (Grant CHE-8620177).

Received July 10th 1992

REFERENCES

- (1) G.R. PETTIT, J.F. DAY, J.L. HARTWELL, H.B. WOOD, *Nature (London)*, 227, 962 (1970).
- (2) G.R. PETTIT, S.B. SINGH, F. HOGAN, P. LLOYD-WILLIAMS, D.L. HERALD, D.D. BURKETT, P.J. CLEWLOW, *J. Am. Chem. Soc.*, 111, 5463 (1989).
- (3) G.R. PETTIT, «Biosynthetic products for cancer chemotherapy», Vol. 1, Plenum Publishing Co., New York, N.Y., 1977.
- (4) G.R. PETTIT, Y. KAMANO, R. AOYAGI, C.L. HERALD, D.L. DOUBEK, J.M. SCHMIDT, J.J. RUDLOE, *Tetrahedron*, 41, 985 (1985).
- (5) G.R. PETTIT, C.L. HERALD, C.R. SMITH, «Biosynthetic products for cancer chemotherapy», Vol. 6, Elsevier Scientific Publishing Co., Amsterdam, 1989.
- (6) G.R. PETTIT, «The Bryostatins», *Progr. Chem. Org. Nat. Prod.*, 57, 153-195 (1991).
- (7) F.J. SCHMITZ, T. YASUMOTO, *J. Nat. Prod.*, 54, 1469 (1991).
- (8) N. FUSEYANI, «Marine metabolites which inhibit development of Echinoderm embryos», *Bioorg. Marine Chem.*, 1, 61 (1987).
- (9) F.E. KOEHN, M. GUNASEKERA, S.S. CROSS, *J. Org. Chem.*, 56, 1322 (1991).
- (10) H.H. SUN, S.S. CROSS, M. GUNASEKERA, F.E. KOEHN, *Tetrahedron*, 47, 1185 (1991).
- (11) A.E. WRIGHT, S.A. RUETH, S.S. CROSS, *J. Nat. Prod.*, 54, 1108 (1991).
- (12) G.R. PETTIT, F. GAO, D. SENGUPTA, J.C. COLL, C.L. HERALD, D.L. DOUBEK, J.M. SCHMIDT, J.R. VAN CAMP, J.J. RUDLOE, R.A. NIEMAN, *Tetrahedron*, 47, 3601 (1991).
- (13) G.R. PETTIT, D.L. HERALD, F. GAO, D. SENGUPTA, C.L. HERALD, *J. Org. Chem.*, 56, 1337 (1991).
- (14) G.R. PETTIT, F. GAO, D.L. HERALD, P.M. BLUMBERG, N.E. LEWIN, R.A. NIEMAN, *J. Am. Chem. Soc.*, 113, 6693 (1991).
- (15) G.R. PETTIT, S.B. SINGH, F. HOGAN, P. LLOYD-WILLIAMS, D.L. HERALD, D.D. BURKETT, P.J. CLEWLOW, *J. Am. Chem. Soc.*, 111, 5463 (1989).
- (16) G.R. PETTIT, S.B. SINGH, F. HOGAN, D.D. BURKETT, *J. Med. Chem.*, 33, 3132 (1990).
- (17) G.R. PETTIT, J. KAMANO, M. INOUE, C. DUFRESNE, M.R. BOYD, C.L. HERALD, J.M. SCHMIDT, D.L. DOUBEK, N.D. CHRISTIE, *J. Org. Chem.*, 57, 429 (1992).
- (18) G.R. PETTIT, C.L. HERALD, M.R. BOYD, J.E. LEET, C. DUFRESNE, D.L. DOUBEK, J.M. SCHMIDT, R.L. CERNY, J.N.A. HOOPER, K.C. RÜTZLER, *J. Med. Chem.*, 34, 3339 (1991).
- (19) R. BAI, K.D. PAULL, C.L. HERALD, L. MALSPEIS, G.R. PETTIT, E. HAMEL, *J. Biol. Chem.*, 266, 15882 (1991).
- (20) G.R. PETTIT, R. TAN, D.L. HERALD, M.D. WILLIAMS, *J. Am. Chem. Soc.*, in preparation.
- (21) G.R. PETTIT, J.A. RIDEOUT, J.A. HASLER, *J. Nat. Prod.*, 44, 588 (1981).
- (22) G.R. PETTIT, C.L. HERALD, J.E. LEET, R. GUPTA, D.E. SCHAUFELBERGER, R.B. BATES, P.J. CLEWLOW, D.L. DOUBEK, K.P. MANFREDI, K. RÜTZLER, J.M. SCHMIDT, L.P. TACKETT, F.B. WARD, M. BRUCK, F. CAMOU, *Can. J. Chem.*, 68, 1621 (1990).
- (23) G.R. PETTIT, P.J. CLEWLOW, C. DUFRESNE, D.L. DOUBEK, R.L. CERNY, K. RÜTZLER, *Can. J. Chem.*, 68, 708 (1990).
- (24) G.R. PETTIT, R. TAN, F. GAO, M.D. WILLIAMS, D.L. DOUBEK, M.R. BOYD, J.M. SCHMIDT, J.C. CHAPUIS, E. HAMEL, J.N.A. HOOPER, *J. Org. Chem.*, in press.
- (25) V.V. MACINTYRE, K.P. SMITH, «New perspectives in sponge biology», K. RÜTZLER, Ed., Proc. 3rd Internat. Sponge Conference, Woods Hole, MA, 1985.
- (26) Y. HIRATA, D. UEMURA, *Pure Appl. Chem.*, 58(5), 701 (1986).
- (27) M.R. BOYD, «Status of the NCI preclinical antitumor drug discovery screen: Implications for selection of new agents for clinical trial», in: «CANCER: Principles and practice of oncology updates», Vol. 3, No. 10, V.T. DEVITA, JR., S. HELLMAN, S.A. ROSENBERG, J.B. LIPPINCOTT, Eds., Philadelphia, 1989, pp. 1-12.
- (28) M.R. BOYD, K.D. PAULL, L.R. RUBINSTEIN, «Data display and analysis strategies for the NCI disease-oriented *in vitro* antitumor drug screen», in «Antitumor drug discovery and development», F.A. VALERIOTE, T. CORBETT, L. BAKER, Eds., Kluwer Academic Publishers, Amsterdam, 1992, pp. 11-34.
- (29) K.D. PAULL, R.H. SHOEMAKER, L. HODES, A. MONKS, D.A. SCUDIERO, L. RUBINSTEIN, J. PLOWMAN, J., M.R. BOYD, *J. Natl. Cancer Inst.*, 81, 1088 (1989).
- (30) A. MONKS, D. SCUDIERO, P. SHEHAN, R. SHOEMAKER, K. PAULL, D. VISTICA, C. HOSE, J. LANGLEY, P. CRONISE, A. VAIGRO-WOLFF, M. GRAY-GOODRICH, H. CAMPBELL, M. BOYD, *J. Natl. Cancer Inst.*, 83, 757 (1991).